MAE 231B Quarter Project
Study of numeric solutions to the equations for exact formulation of non-scattering radiative transfer equation for one-dimensional, parallel plates and the equation of the Rosseland diffusion approximation for equal nondimensional conduction-to-radiation parameter values

Jon Van Lew

December 9, 2010

Contents

1 Introduction

In the study of combined conduction and radiation an extremely convenient model is to apply the Rosseland approximation which essentially allows one to treat radiation heat transfer in the same manner as Fourier's law of heat diffusion. The Rosseland approximation was derived under the considerations of an "optically thick" medium (optical thickness will be explicitly shown later). In this study, we will solve for the temperature profile in one-dimensional medium between infinite, black parallel plates which are held at constant temperature. The solution will be found via considerations of the full radiative transfer equation as well as with application of the Rosseland approximation.

The equations for the radiative transfer equation and Rosseland approximation will be reduced into non-dimensional form and it will be shown that they are both functions of a single dependent variable, N, which we will define as the ratio of conduction to radiation through the medium; and a single independent variable τ the optical depth. The reduction will allow for a straightforward parametric study between the solutions of the two methods. Through the comparison of the two methods, we can ultimately conclude under conditions the applicability of the Rosseland approximation is appropriate.

2 Analysis

2.1 Schematic

The medium will be of thickness L along the z-axis between two infinite parallel plates emitting as black bodies as shown in Fig. 1.

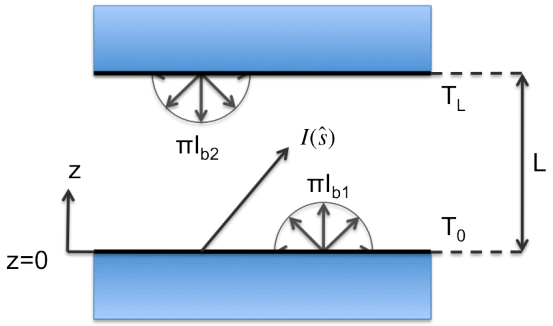

Figure 1: Schematic drawing of one-dimensional black, parallel plates

2.2 Assumptions

We will assume that the medium being irradiated will not experience internal bouyant forces due to differences in density from temperature gradients. This removes internal mixing and natural convection of the fluid. Furthermore, the following assumptions will be made in the study.

- Isotropically scattering medium and non-scattering medium in the Rosseland approximation and radiative transfer equation formulations, respectively.
- Optically thick medium in the Rosseland approximation formulation.
- Medium is grey.
- One-dimensional.
- Bounded by isothermal, isotropic, gray, diffusely emitting and reflecting walls.
- Homogenous medium (i.e. constant properties).
- Steady state.

2.3 Governing Equations

2.3.1 Energy Conservation Equation

The general energy conservation equation for conduction and radiation is

$$\rho c \frac{\partial T}{\partial t} = \nabla \cdot (k_c \nabla T) - \nabla \cdot q_R + \dot{q}_g \tag{1}$$

where ρ, c and k_c are the density, specific heat, and thermal conductivity of the medium, respectively; T is the temperature of the medium; and q_R is the radiative heat transfer rate. The thermal conductivity we will assume to be constant over the temperature ranges considered in this study. We will consider a system where there is no heat generation and therefore $\dot{q}_g$ will be disregarded.

For a one-dimensional, steady state consideration this is

$$0 = \frac{d}{dz}\left(k_c \frac{dT}{dz}\right) - \frac{dq_R}{dz} \tag{2}$$

With a knowledge of the divergence radiative heat transfer q_R we would be capable of finding the temperature field along z from Eq. (2). The radiative heat transfer flux is connected to the radiative transfer equation (RTE) which must be solved concurrently. As mentioned, in this paper we will consider solutions to the Eq. (2) as sought from the i) RTE formulation and ii) from the simplification which allows us to treat the radiation transfer as a simple diffusion process.

2.3.2 Radiative Transfer Equation

Before beginning discussions of the divergence of the radiative heat flux, we must address the energy balance for thermal radiation. It can be shown that the equation of transfer is

$$\frac{1}{c}\frac{\partial I}{\partial t} + \hat{s} \cdot \nabla I = -\kappa I + \kappa I_b - \sigma_s I + \frac{\sigma_s}{4\pi} \iint_{4\pi} \Phi(\hat{s}_i, \hat{s}) I(\hat{s}_i)\, \mathrm{d}\Omega_i \tag{3}$$

in quasi-steady form this can be expressed as

$$\hat{s} \cdot \nabla I = -\beta I + \kappa I_b + \frac{\sigma_s}{4\pi} \iint_{4\pi} \Phi(\hat{s}_i, \hat{s}) I(\hat{s}_i)\, \mathrm{d}\Omega_i \tag{4}$$

For brevity, details of the solution (as it was derived in the class notes) for one-dimensional medium will be omitted. We introduce the optical depth, τ; defined as $\tau = \int_0^z \beta \, \mathrm{d}z$ (or $\tau = \beta z$ for uniform medium). When referring to optical thickness we will be considering the optical depth at z-location L, or τ_L. The intensity in terms of τ is then

$$I(\tau) = I_0 e^{-\tau} + \int_0^\tau S(\tau', \hat{s}) e^{-(\tau - \tau')} \, \mathrm{d}\tau' \tag{5}$$

where the source term on the right is

$$S(\tau', \hat{s}) = (1 - \omega) I_b(T) + \frac{\omega}{4\pi} \iint_{4\pi} \Phi(\hat{s}_i, \hat{s}) I(\hat{s}_i) \, \mathrm{d}\Omega_i \tag{6}$$

However, rather than considering an isotropically scattering medium as we will when working with the Rosseland approximation (discussed in Appendix A), we will begin the study by assuming that the medium is non-scattering, where $S(\tau') = I_b(\tau')$ and therefore a direct solution to Eq. (4) can be calculated from

$$I(\tau) = I_0 e^{-\tau} + \int_0^\tau I_b(\tau') e^{-(\tau - \tau')} \, \mathrm{d}\tau' \tag{7}$$

and it follows that an exact solution to Eq. (2) can also be determined.

2.3.3 Divergence of Radiative Heat Transfer Rate

Following [1], and with details in Appendix A and B, it can be shown that the radiative heat transfer q_R in terms of the optical depth and optical thickness can be expressed as

$$q_R(\tau) = 2J_1 E_3(\tau) - 2J_2 E_3(\tau_L - \tau) + 2\pi \int_0^\tau I_b(\tau') E_2(\tau - \tau') \, \mathrm{d}\tau' - 2\pi \int_\tau^{\tau_L} I_b(\tau') E_2(\tau' - \tau) \, \mathrm{d}\tau' \tag{8}$$

The boundary conditions of $T(\tau_0) = T_0$ and $T(\tau_L) = T_L$ will be fed into the both the energy balance as well as the radiative heat transfer divergence equation in the form of black body intensity. We can numerically solve Eq. (8) with a guess at the temperature field along τ which, after calculated, will allow a solution to be numerically calculated for Eq. (2).

2.3.4 Optically-Thick Heat Transfer Rate

For a one-dimensional, optically thick, isotropically scattering medium, the radiative heat flux is

$$q_R = -\frac{4\sigma}{3\beta_R} \frac{d(n^2 T^4)}{dz} \tag{9}$$

where β_R is the Rosseland-mean extinction coefficient. This form of the equation is also valid for a nonscattering medium. In a nonscattering medium, the scattering coefficient inside β_R vanishes and we may treat β_R as κ_R. In the form above, it is apparent that we may treat the problem as one of pure diffusion by expressing the radiative heat flux as

$$q_R = -k_R \frac{dT}{dz} \tag{10}$$

where

$$k_R = \frac{16n^2\sigma T^3}{3\beta_R} \tag{11}$$

Thus for a one-dimensional, steady state consideration, Eq. (1) becomes

$$0 = \frac{d}{dz}\left(k_c\frac{dT}{dz} + k_R\frac{dT}{dz}\right) \tag{12}$$

with equivalent boundary conditions from the RTE formulation

$$T(z_0) = T_0 \qquad\qquad T(z_L) = T_L$$

2.4 Method of Solution

From Eq. (8) and Eq. (12) we are capable of deducing temperature fields through the medium for i) solution of the RTE for a nonscattering medium and ii) implementation of the Rosseland approximation, respectively. Numeric schemes will be implemented to solve both of these equations.

For numeric solution at discrete nodes, we can express Eq. (8) at every node as a summation over all nodes from τ_0 to τ_L [1]. With $\frac{dq_R}{d\tau}$ calculated, we will use a tridiagonal matrix solver developed by the author to find temperature for the boundary value problem (See Appendix C).

A direct solution to Eq. (12) can be found from a numeric schemes to solve the 2nd order ODE with code employing Huen's method and an adaptive timestep; also developed by the author. We can solve this ODE with knowledge of the two prescribed boundary conditions of constant temperature at the surfaces.

A parametric study of the two solutions should then show when the Rosseland approximation is appropriate and for what conditions of optical depth it should be considered valid.

2.4.1 Numeric Solution to the RTE-derived Energy Conservation Equation

Using optical thickness we can write Eq. (2) as

$$0 = \beta k_c\frac{d^2T}{d\tau^2} - \frac{dq_R}{d\tau} \tag{13}$$

where for a nonscattering medium $\beta = \kappa$ and $\sigma_s = 0$.

We introduce the nondimensional temperature and heat flux

$$\theta = \frac{T}{T_0} \qquad\qquad \Psi = \frac{q_R}{n^2\sigma T_0^4} \tag{14}$$

and

$$d^2T = T_0 d^2\theta \tag{15}$$

Plugging the nondimensional variables then integrating by parts, introducing the Liebnitz rule[1], and assuming black boundaries it can be shown that the divergence of the nondimensional radiative heat flux is

$$\frac{d\Psi}{d\tau} = 2\left\{\int_0^\tau \frac{d\theta^4}{d\tau}E_2(\tau-\tau')\,\mathrm{d}\tau - \int_\tau^{\tau_L}\frac{d\theta^4}{d\tau}E_2(\tau'-\tau)\,\mathrm{d}\tau\right\} \tag{16}$$

By dividing the coefficient of the conduction term by the common coefficient before the two radiation terms will give a dimensionless parameter indicating which mode of heat transfer dominates in a given situation. This parameter is defined as N which is

$$N = \frac{k_c \kappa}{4n^2 \sigma T_0^3} \tag{17}$$

We do the division of radiation coefficient from conduction coefficient to find

$$0 = 4N \frac{d^2\theta}{d\tau^2} - \frac{d\Psi}{d\tau} \tag{18}$$

From the RTE, with no scattering, the energy conservation can be seen as a linear second order ODE; this allows the implementation of relatively straightforward numeric solver. The boundary conditions imposed on it are known temperature at τ_0 and τ_L; it is a boundary value problem (BVP). The details of the tridiagonal solver are lengthy and omitted. They are included for reference in Appendix C.

2.4.2 Numeric Solution to the Rosseland Approximation

To solve the energy conservation equation derived from the Rosseland approximation we first expand Eq. (12) to

$$0 = k_c \frac{d^2T}{dz^2} + \left(\frac{dT}{dz} \frac{dk_R}{dT} \right) \frac{dT}{dz} + k_R \frac{d^2T}{dz^2} \tag{19}$$

$$0 = k_c \frac{d^2T}{dz^2} + \frac{dk_R}{dT} \left(\frac{dT}{dz} \right)^2 + k_R \frac{d^2T}{dz^2} \tag{20}$$

$$0 = k_c \frac{d^2T}{dz^2} + \frac{16n^2\sigma T^2}{\beta_R} \left(\frac{dT}{dz} \right)^2 + \frac{16n^2\sigma T^3}{3\beta_R} \frac{d^2T}{dz^2} \tag{21}$$

We introduce the non-dimensional variables for temperature and the optical thickness as discussed above

$$0 = k_c T_0 \beta_R^2 \frac{d^2\theta}{d\tau^2} + \frac{16n^2\sigma T_0^3}{\beta_R} T_0 \beta_R^2 \theta^2 \left(\frac{d\theta}{d\tau} \right)^2 + \frac{16n^2\sigma T_0^3}{3\beta_R} T_0 \beta_R^2 \theta^3 \frac{d^2\theta}{d\tau^2} \tag{22}$$

$$0 = k_c \frac{d^2\theta}{d\tau^2} + \frac{16n^2\sigma T_0^3}{\beta_R} \theta^2 \left(\frac{d\theta}{d\tau} \right)^2 + \frac{16n^2\sigma T_0^3}{3\beta_R} \theta^3 \frac{d^2\theta}{d\tau^2} \tag{23}$$

We again introduce the same conduction to radiation ratio, N, as given above (substituting β_R for κ.) Performing the non-dimensionalization and Eq. (23) is

$$0 = \frac{k_c \beta_R}{4n^2\sigma T_0^3} \frac{d^2\theta}{d\tau^2} + 4\theta^2 \left(\frac{d\theta}{d\tau} \right)^2 + \frac{4}{3} \theta^3 \frac{d^2\theta}{d\tau^2} \tag{24}$$

$$0 = N \frac{d^2\theta}{d\tau^2} + 4\theta^2 \left(\frac{d\theta}{d\tau} \right)^2 + \frac{4}{3} \theta^3 \frac{d^2\theta}{d\tau^2} \tag{25}$$

However, the Rosseland approximation has introduced nonlinearity to the 2nd order ODE. Therefore, in order to solve the equation numerically we will reduce it to a system of first order ODEs resembling an initial value problem (IVP). To create a system of equations, we introduce new variable, $\vec{u}$ where the constituents are

$$u_1 = \theta \tag{26}$$

$$u_2 = \frac{du_1}{d\tau} = \frac{d\theta}{d\tau} \tag{27}$$

therefore (after rearranging Eq. (25))

$$\frac{d\vec{u}}{d\tau} = \vec{F}(\vec{u}) \tag{28}$$

$$\frac{d}{d\tau}\begin{bmatrix} u_1 \\ u_2 \end{bmatrix} = \begin{bmatrix} u_2 \\ -4u_1^2 \\ \hline N + \frac{4}{3}u_1^3 \end{bmatrix} u_2^2 \tag{29}$$

with initial conditions

$$\vec{u}_0 = \begin{pmatrix} \theta_0 \\ \frac{d\theta}{d\tau}|_0 \end{pmatrix} \tag{30}$$

We will use Huen's method, defined as

$$\vec{u}_i = \vec{u}_{i-1} + \frac{h}{2}\vec{F}(\vec{u}_{i-1}) + \frac{h}{2}\vec{F}(\vec{u}_{i-1} + h\vec{F}(\vec{u}_{i-1})) \tag{31}$$

as the numeric scheme. The method will proceed from $i = 1, 2, \ldots, M$, where $M = 1/h$ to span $\tau \in [\tau_0, \tau_L]$. h is the chosen step size for the numeric method to satisfy stability concerns for the ODE being analyzed.

To solve the IVP we see from Eq. (30) that a "known" temperature gradient at τ_0 is required in addition to the known temperature. Of course, we do not know the gradient at this location a priori and must determine this with an iterative scheme. To begin, we guess some value for the temperature gradient. Knowing this value will allow the numeric scheme to proceed from τ_0 up to τ_L where the temperature will be calculated. The numeric value, θ_L^k, will be compared to the known value, θ_L, as given by the boundary conditions. If they are different, knowledge of the value will inform the next chosen iteration, $k = k + 1$, of temperature gradient at τ_0 and the numeric method is run again; this is known as "shooting." The shooting method will iterate until the value of θ_L^k converges to θ_L.

2.4.3 Solution Procedures

Finding the temperature distribution with conduction and radiation without scattering results in a linear equation for the RTE-based derivation and non-linear equation for the Rosseland approximation. The temperature dependence of radiation is to the fourth power and the dependence on conduction is linear. The non-linear temperature field must therefore be determined from an

iterative procedure for both of the solutions outlined in this paper. The processes are similar but involve one extra step of iteration in the RTE method.

This iterative procedure for the RTE-derived solution will proceed as following

1. Guess a temperature field.
2. Determine nondimensionalized divergence of radiation heat flux Ψ, as predicted by the RTE.
3. Solve the nondimensionalized conservation of energy equation with the derived value of radiative heat flux.
   (a) Run the tridiagonal solver outlined in Appendix C with $A = 1$ and $D = \frac{1}{4N}\frac{d\Psi}{d\tau}\Big|_i$
   (b) Find a temperature field from the solution of the conservation of energy.
4. Compare the new temperature field from the previous (or guessed) temperature field. Repeat until the calculated temperature field matches the previous temperature field in some prescribed way.

The procedure to find the temperature distribution for the assumption of optically thick proceeds in much the same way. We have reduced the 2nd order ODE BVP into a system of 1st order IVP which will be solved with the "shooting" technique.

1. Solve the nondimensionalized conservation of energy equation with the derived value of radiative heat flux.
   (a) Do a "shooting" iteration on the IVP system of equations based on the 2nd order BVP
   (b) Find a temperature field from the solution of the conservation of energy.

3 Results and Discussion

3.1 RTE Approximation

The RTE equations were placed into the tridiagonalization solving routine to find temperature with $\tau \in [0, 1]$. The results are shown in Fig. (2). There were problems implementing the code necessary to solve for the smallest values of N when the temperature profile is totally dominated by radiation. For this reason, I could find converging results for temperature for $N > 10^{-1}$.

The temperature profile from the RTE-derived equations were again solved, this time along $\tau \in [0, 2]$ and $\tau \in [0, 10]$. The results are given in Fig. (3) and Fig. (5). Again there were problems implementing the code for small values of N and the converged results were all out of the domain of the problem. The only reliable results came with parametric values of $N > 10^0$. Though these values still give an indication of answers for the RTE to be compared with the Rosseland approximation.

3.2 Rosseland Approximation

We solve Eq. (29) over $\tau \in [0, 1]$, choosing $\theta_L = 1$, and specify a variety of radiation-conduction ratio parameters $N = 10^j$ for $j = -2, -1, \ldots, 2$. When N is small we expect radiation to dominate as the contribution to temperature is scaled by $1/N$ and we likewise expect conduction to dominate as N gets larger. This is precisely what we see in Fig. (2). For the values of $N = 10^{-2}$ and $N = 10^{-1}$, the

nonlinear radiation trend dominates over the linear conduction influence. For $N = 10^0$ to $N = 10^2$ the curves have tended toward the linear conduction result.

We repeat the process with $\tau \in [0, 2]$ and $\tau \in [0, 10]$. The same behavior is seen for increasing values of N. The results are given in Fig. 3, Fig. 4, and Fig. 5, respectively. We also increase $\theta_L = 5$ to and run it for optical depth to $\tau_L = 1$. In Fig. 6 we can see how little the Rosseland approximation agrees with the two solution curves found for the RTE.

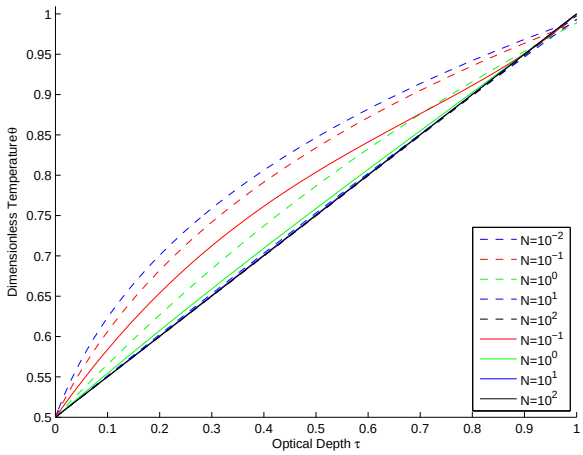

Figure 2: Rosseland diffusion approximation for combined conduction and radiation with $\theta_0 = 0.5$, $\theta_L = 1$, $\tau_L = 1$

4 Conclusion

For very small N the radiation contribution to the temperature profile is most noticeable. The temperature's fourth order dependence on radiation heat transfer ensures a non-linear profile through the axis of interest. At increasing values of N the influence of conduction increases until eventually a linear profile dominates the solution. This behavior was observed for both the RTE formulation of the equations as well as the Rosseland approximation.

We can compare the RTE formulated results in Fig. (2) to Rosseland approximation and see that for the N values computed, the error of the Rosseland approximation is fairly pronounced. Had we shrank τ_L further, this discrepancy would be even greater.

In Fig. 3 we see that the RTE formulated and Rosseland approximated solutions begin to match slightly better. Yet there as N shrinks (i.e. radiation becomes the dominant mode of heat transfer), the error in the diffusion approximation begins to increase. Increasing τ_L all the way to $\tau_L = 10$, however, showed that the Rosseland approximation is already approaching a qualitatively correct solution in comparison to the RTE formulation. In Fig. (5), the curves for computed values of N match well over the span of τ.

The Rosseland approximation was derived under the assumption that the optical thickness was

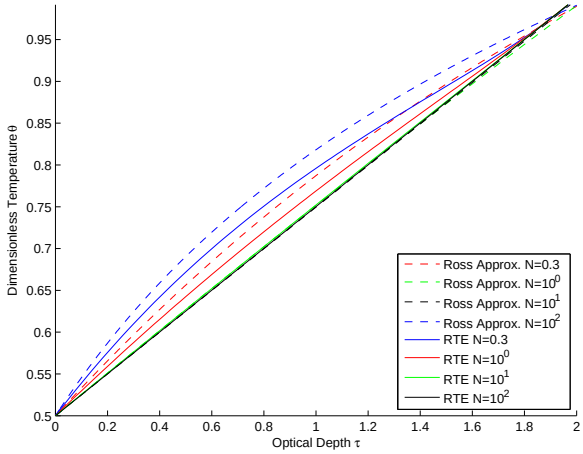

Figure 3: Rosseland diffusion approximation for combined conduction and radiation with $\theta_0 = 0.5$, $\theta_L = 1$, $\tau_L = 2$

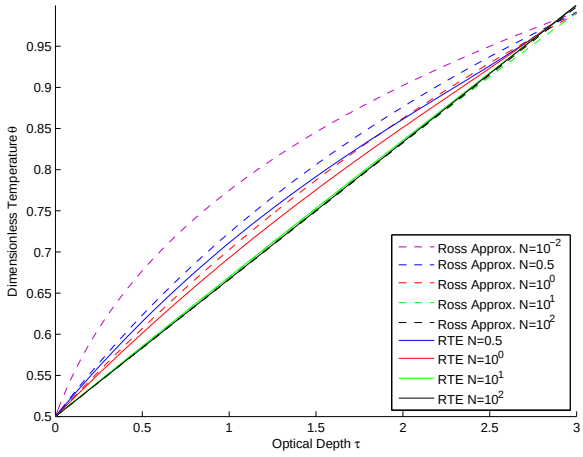

Figure 4: Rosseland diffusion approximation for combined conduction and radiation with $\theta_0 = 0.5$, $\theta_L = 1$, $\tau_L = 3$

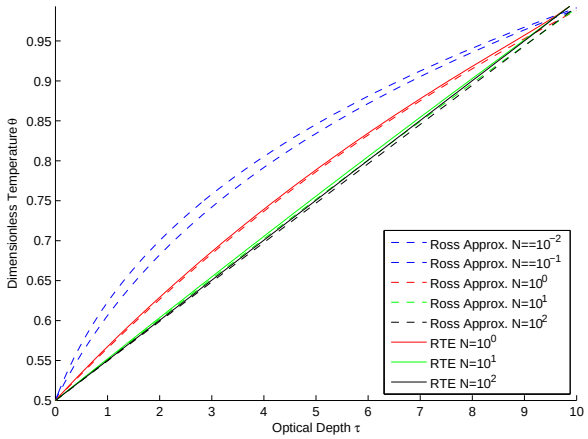

Figure 5: Rosseland diffusion approximation for combined conduction and radiation with $\theta_0 = 0.5$, $\theta_L = 1$, $\tau_L = 10$

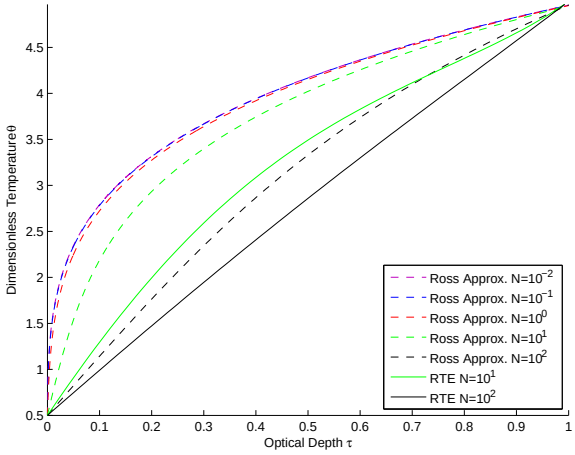

Figure 6: Rosseland diffusion approximation for combined conduction and radiation with $\theta_0 = 0.5$, $\theta_L = 5$, $\tau_L = 1$

very large, $\tau_L \gg 1$. This assumption allowed for simplification of the source term in the RTE in such a way that the divergence of the heat transfer flux could be expressed effectively as a diffusion problem similar to Fourier's law of heat conduction.

In the Bier-Lambert law it is known that when $\tau_L = 3$ as much as 95% of the original signal has been absorbed/single-scattered through the medium. This had implied to me that $\tau_L = 3$ may be sufficiently "thick" from the standpoint of applicability of the Rosseland approximation. Yet we see in Fig. 4 that there is still considerable mismatch between the results of the Rosseland approximation and the RTE formulation.

From the results of this study it appears that for $\tau_L > 10$ the Rosseland approximation is applicable if θ_L/θ_0 is not too large. However, this result is under the condition that the trends seen in Fig. 5 continue for ever-decreasing values of N. Given more time, the bugs in the code could be worked out for the method of solution for $N < 1$ and this assumption could be verified or rejected. Regardless, we have confirmed that the Rosseland approximation is valid under certain conditions of N for an optical thickness of $\tau_L = 10$ but should be implemented with caution for optical thicknesses of the order of $\tau_L < 5$. Furthermore, as evidenced in Fig. 6 the size of θ_L/θ_0 is also important in the accuracy of the Rosseland approximation. The discrepancies in solutions between the RTE formulation and the Rosseland approximation have been magnified at a large ratio of dimensionless temperatures at the boundaries.

A Irradiation derivation

A somewhat simple solution can be obtained when we consider an isotropically scattering medium. This assumption allows us to approach a solution without implementing Mie Theory on particles of specific shapes. We can say that the radius of whatever particle under consideration is $r \ll \lambda$ to make the assumption valid. For an isotropically scattering medium, $\Phi \equiv 1$, therefore the source term S becomes

$$S(\tau', \hat{s}) = (1-\omega) I_b(T) + \frac{\omega}{4\pi} G(\tau') \tag{32}$$

Noting that in the isotropic case, the source is independent of direction, $\hat{s}$. The irradiation, G is defined as the total incident radiation flux at a point in space.

$$G(\tau) = \iint_{4\pi} I(\tau, \theta)\, \mathrm{d}\Omega \tag{33}$$

for solid angle $\mathrm{d}\Omega = sin\theta\, \mathrm{d}\theta\, \mathrm{d}\phi$.

The irradiation, as given in Eq. (33) can be expanded in terms of our derived values of intensity (given in Eq. (7).) The irradiation will be given in terms of the intensity for a one-dimensional grey medium between two infinite parallel plates. Introducing the direction cosine, $\mu = cos\theta$, and the irradiation in terms of τ is

$$\begin{aligned} G(\tau) =& 2\pi \Bigg\{ I_{b1} \int_0^1 e^{-\tau/\mu}\, \mathrm{d}\mu + I_{b2} \int_0^1 e^{-(\tau_L - \tau)/\mu}\, \mathrm{d}\mu + \\ &+ \int_0^\tau I_b(\tau') \int_0^1 e^{-(\tau-\tau')/\mu} \frac{\mathrm{d}\mu}{\mu} \mathrm{d}\tau' + \int_\tau^{\tau_L} I_b(\tau') \int_0^1 e^{-(\tau'-\tau)/\mu} \frac{d\mu}{\mu} \mathrm{d}\tau' \Bigg\} \end{aligned} \tag{34}$$

Following the notation given in [1] we introduce the *exponential integral of order n*,

$$E_n(x) = \int_0^1 \mu^{n-2} e^{-x/\mu}\, \mathrm{d}\mu \tag{35}$$

This function is built into MATLAB and will assist in the numeric solution of $G(\tau)$. We can express Irradiation as

$$G(\tau) = 2\pi \left\{ \frac{n^2 \sigma T_0^4}{\pi} E_2(\tau) + \frac{n^2 \sigma T_L^4}{\pi} E_2(\tau_L - \tau) + \int_0^\tau \frac{n^2 \sigma T^4}{\pi} E_1(\tau - \tau')\, \mathrm{d}\tau' + \int_\tau^{\tau_L} \frac{n^2 \sigma T^4}{\pi} E_1(\tau' - \tau)\, \mathrm{d}\tau' \right\} \tag{36}$$

$$G(\tau) = 2n^2 \sigma T_0^4 \left\{ E_2(\tau) + \frac{T_L^4}{T_0^4} E_2(\tau_L - \tau) + \int_0^\tau \frac{T^4}{T_0^4} E_1(\tau - \tau')\, \mathrm{d}\tau' + \int_\tau^{\tau_L} \frac{T^4}{T_0^4} E_1(\tau' - \tau)\, \mathrm{d}\tau' \right\} \tag{37}$$

Observing $\int_0^x E_n(x-z)\, \mathrm{d}z = 1 - E_{n+1}(x)$ and $\int_x^{x_L} E_n(z-x)\, \mathrm{d}z = 1 - E_{n+1}(x_L - x)$ we can find an explicit form of G

$$G(\tau) = 2n^2 \sigma T_0^4 \left\{ E_2(\tau) + \frac{T_L^4}{T_0^4} E_2(\tau_L - \tau) + \frac{T^4}{T_0^4}(1 - E_2(\tau)) + \frac{T^4}{T_0^4}(1 - E_2(\tau_L - \tau)) \right\} \tag{38}$$

The terms in the radiosity equation can be found for specific cases of known boundaries and the integrals of the exponentials can be calculated at every location τ.

In non dimensional form the irradiation is (noting that $\theta_0 \equiv 1$).

$$4n^2\sigma T_0^4\, g(\tau) = 2n^2\sigma T_0^4 \left\{ E_2(\tau) + \theta_L^4 E_2(\tau_L - \tau) + \int_0^\tau \theta^4 E_1(\tau - \tau')\,\mathrm{d}\tau' + \int_\tau^{\tau_L} \theta^4 E_1(\tau' - \tau)\,\mathrm{d}\tau' \right\} \tag{39}$$

$$g(\tau) = \frac{1}{2}\left\{ E_2(\tau) + \theta_L^4 E_2(\tau_L - \tau) + \int_0^\tau \theta^4 E_1(\tau - \tau')\,\mathrm{d}\tau' + \int_\tau^{\tau_L} \theta^4 E_1(\tau' - \tau)\,\mathrm{d}\tau' \right\} \tag{40}$$

B Divergence of radiative heat transfer derivation

We start from the energy balance established in Eq. (4) and we integrate over all solid angles to find

$$\iint_{4\pi} \hat{s}\cdot\nabla I\,\mathrm{d}\Omega = \iint_{4\pi} -\beta I\,\mathrm{d}\Omega + \iint_{4\pi} \kappa I_b\,\mathrm{d}\Omega + \iint_{4\pi} \frac{\sigma_s}{4\pi} \iint_{4\pi} \Phi(\hat{s}_i,\hat{s}) I(\hat{s}_i)\,\mathrm{d}\Omega_i\,\mathrm{d}\Omega \tag{41}$$

$$\nabla\cdot \iint_{4\pi} I\hat{s}\,\mathrm{d}\Omega = \iint_{4\pi} -\beta I\,\mathrm{d}\Omega + \iint_{4\pi} \kappa I_b\,\mathrm{d}\Omega + \iint_{4\pi} \frac{\sigma_s}{4\pi} \iint_{4\pi} \Phi(\hat{s}_i,\hat{s}) I(\hat{s}_i)\,\mathrm{d}\Omega_i\,\mathrm{d}\Omega \tag{42}$$

$$\nabla\cdot q_R = \iint_{4\pi} -\beta I\,\mathrm{d}\Omega + 4\pi\kappa I_b + \frac{\sigma_s}{4\pi} \iint_{4\pi} I(\hat{s}_i) \left(\iint_{4\pi} \Phi(\hat{s}_i,\hat{s})\,\mathrm{d}\Omega \right) \mathrm{d}\Omega_i \tag{43}$$

$$\nabla\cdot q_R = -\beta \iint_{4\pi} I\,\mathrm{d}\Omega + 4\pi\kappa I_b + \sigma_s \iint_{4\pi} I(\hat{s}_i)\,\mathrm{d}\Omega_i \tag{44}$$

Because $\mathrm{d}\Omega_i$ is just a dummy variable for $\mathrm{d}\Omega$, we can combine the two integrals on the right hand side as

$$\nabla\cdot q_R = 4\pi\kappa I_b - \kappa \iint_{4\pi} I\,\mathrm{d}\Omega \tag{45}$$

$$\nabla\cdot q_R = \kappa(4\pi I_b - G) \tag{46}$$

knowing the heat flux q_R is

$$q_R = \iint_{4\pi} I\,\hat{s}\,\mathrm{d}\Omega \tag{47}$$

Equation (46) provides the divergence of the radiative heat transfer rate where κ is the absorptive coefficient of the medium; I_b is the radiative intensity of a black body at the temperature T of the medium; and $G(z)$ is the irradiation of the medium at the location z.

In one dimension for a grey medium this is just

$$\frac{dq_R}{dz} = \kappa(4\pi I_b - G(z)) \tag{48}$$

where σ is the Stefann-Boltzman constant.

In terms of the optical thickness, the divergence is

$$\frac{dq_R}{d\tau} = (1-\omega)(4n^2\sigma T^4 - G(\tau)) \tag{49}$$

The black body intensity, I_b can be determined directly from knowledge of the temperature as it is simply $I_b = n^2\sigma T^4/\pi$. We now turn our attention to the irradiation term. The irradiation has been given in Eq. (37). Thus we have all terms necessary to solve Eq. (2). We plug Eq. (49) back into the energy balance to find

$$0 = \frac{d}{d\tau}\left(\beta k_c \frac{dT}{d\tau}\right) - (1-\omega)(4n^2\sigma T^4 - G(\tau)) \tag{50}$$

C Tridiagonal solver

The tridiagonal solver was designed to solve an ODE of the form

$$A(x)\frac{d^2y}{dx} + B(x)\frac{dy}{dx}C(x)y = D(x) \quad \text{with } y(x) \text{ on } x_1 \le x \le x_2 \tag{51}$$

Rearranging Equation 51 to have all terms other than the second order derivative on the right-hand side

$$\frac{d^2y}{dx} = -\frac{B(x)}{A(x)}\frac{dy}{dx} - \frac{C(x)}{A(x)}y + \frac{D(x)}{A(x)} \tag{52}$$

The corresponding numeric form of the equation is then (after rearranging)

$$\big[1 - \frac{hC_i}{2A_i}\big]y_{i-1} + \big[\frac{hC_i}{2A_i} - 2\big]y_i + \big[1 + \frac{hB_i}{2A_i}\big]y_{i+1} = h^2\frac{D_i}{A_i} \tag{53}$$

Where $A_i = A\big(x(i)\big)$, etc.. It must be noted that this solver is established to solve 2nd order ordinary differential equations, as such $A(x)$ is assumed to be $\neq 0$. In the case that $A(x) = 0$ simple modifications are made to the coefficients to avoid *division by* 0.

C.1 Matrix Form Solution: Tridiagonal Solver Algorithm

To solve any of the above types of boundary value problems we will implement the same form of a tridiagonal matrix algorithm solution (or Thomas algorithm). With the given boundaries of all types, and with the central difference method applied to the ODE we are left with a tridiagonal matrix. This matrix is solved with essentially the same algorithm in all cases with only minor modifications required. The coefficients of Equation 53, when $i = 1, 2, \ldots, n$ yield $n-1$ equations. The matrix form of these $n-1$ equations is

$$\begin{pmatrix} b_1 & c_1 & \cdots & \cdots & 0 \\ a_2 & b_2 & c_2 & \cdots & \vdots \\ 0 & a_3 & b_3 & c_3 & \vdots \\ \vdots & \vdots & \vdots & \ddots & c_{n-2} \\ 0 & \cdots & \cdots & a_{n-1} & b_{n-1} \end{pmatrix} * \begin{pmatrix} y_1 \\ \vdots \\ \vdots \\ y_{n-2} \\ y_{n-1} \end{pmatrix} = \begin{pmatrix} d_1 \\ \vdots \\ \vdots \\ d_{n-2} \\ d_{n-1} \end{pmatrix}$$

Where

$$a_i = 1 - \frac{hC_i}{2A_i} \qquad i = 2, 3, \ldots, n-1$$
$$b_i = \frac{hC_i}{2A_i} - 2 \qquad i = 1, 2, \ldots, n-1$$
$$c_i = 1 + \frac{hB_i}{2A_i} \qquad i = 1, 2, \ldots, n-2$$

$$d_i = \begin{cases} h^2 D_1/A_1 - a_1 y_0 & i = 1 \\ h^2 D_i/A_i & i = 2, 3, \ldots, n-2 \\ h^2 D_{n-1}/A_{n-1} - c_{n-1} y_n & i = n-1 \end{cases}$$

The solution, via the tridiagonal matrix algorithm, is only valid when $|b_i| > |a_i| + |c_i|$ for all $i = 1, 2, ..n$. If this is satisfied, the matrix is referred to as being *diagonally dominant*. This depends entirely on the given ODE and is infrequently seen but must be taken into account before the solution is run.

If the BVP is Dirichlet-type, the coefficients of a_1 and c_n are simply specified by the boundary conditions. This will leave us with, including the matrix of equations, $n+1$ equations and $n+1$ unknowns.

D Tridiagonalization code for solving RTE

```
% Jon Van Lew 2010
clear all; close all; clc;
j=-1;
N   = 10^j;
i=1;
M=101;
h=10/(M-1);
y(1)=.5;
y(M)=1;
x(1)=0;
x(M)=10;

Tg   = zeros(M,1);

% for i=1:M
%     Tg(i,1)= (y(M)-y(1))/(M-1)*(i-1)+y(1);
% end
load('Tg')

ep=1;

while ep>.001;
    for i=2:M-1;
```

```
    rhs=0;
    for j=2:M
        rhs = rhs+(Tg(j,1)^4 - Tg(j-1,1)^4)*(mfun('Ei',3,abs(i-j)*h)-mfun('Ei',3,abs(i+1-j)*h));
    end
    dpsidtau(i-1) = (2/h)*rhs;

    x(i)=(i-1)*h;


    if i==2
        bb(i)=h^2*C(x(i))/A(x(i))-2;
        cc(i)=1+(h*B(x(i)))/(2*A(x(i)));
        dd(i)=(h^2*D(x(i),dpsidtau(i-1),N)/A(x(i)))-(1-(h*B(x(i)))/(2*A(x(i))))*y(1);
    elseif i==M-1
        aa(i)=1-(h*B(x(i)))/(2*A(x(i)));
        bb(i)=h^2*C(x(i))/A(x(i))-2;
        dd(i)=(h^2*D(x(i),dpsidtau(i-1),N)/A(x(i)))-((1+(h*B(x(i)))/(2*A(x(i)))))*y(M);
    else
        aa(i)=1-(h*B(x(i)))/(2*A(x(i)));
        bb(i)=h^2*C(x(i))/A(x(i))-2;
        cc(i)=1+(h*B(x(i)))/(2*A(x(i)));
        dd(i)=h^2*D(x(i),dpsidtau(i-1),N)/A(x(i));
    end

    %updated elements
    if i==2
        cc(i)=cc(i)/bb(i);
        dd(i)=dd(i)/bb(i);
    elseif i<M-1
        cc(i)=cc(i)/(bb(i)-cc(i-1)*aa(i));
        dd(i)=(dd(i)-dd(i-1)*aa(i))/(bb(i)-cc(i-1)*aa(i));
    else
        dd(i)=(dd(i)-dd(i-1)*aa(i))/(bb(i)-cc(i-1)*aa(i));
    end
end


y(M-1)=dd(M-1);
for i=M-2:-1:2;
    y(i)=dd(i)-cc(i)*y(i+1);
end

T=y;

ep=abs(Tg((M-1)/2) - T((M-1)/2));
```

```
    Tg=T';
    break
end

plot(x,y)
```

E MATLAB code for Rosseland Approximation using adaptive timestep

```
% Jon Van Lew 2010
% Adaptive timestep with Huen's method for finding the temperature
% distribution along dimensionless z with combined conduction and radiation
% as specified by parameter N

clear all; clc; close all; format compact; format long;
figure(1)
hold on
% The values of qiv were determined from earlier guesses at qi for each
% value of j.  This gives a good starting point so the convergence
% iteration below can find a solution quickly.
%qiv     = [1.74187896527146,1.30357003354641,0.674492882220646,0.515023265146478,0.500000000000000;

p       = 1;
TL=1;
tauL    = 10;
tau0    = 0;
eta=10^-3;
z=0;
h   = .5;
Ti  = .5;
for j=-2:1:2
    N   = 10^j;

    %qi  = qiv(p);
    qi=(TL-Ti)/(tauL-tau0);
    ep  = 1;

    while ep > 0.01
        %M      = (tauL-tau0)/h+1;
        v      = zeros(1,3);
        v(1,:) = [Ti qi tau0];
        i=1;
        z=0;
        % for i=2:M
        while z<tauL
```

```
            i=i+1;
            vs = huen(v(i-1,:),h,N);
            vh(1,:) = huen(v(i-1,:),h/2,N);
            vh2(1,:) = huen(v(i-1,:),h/2,N);
            z=vh2(1,3);

            % Adaptive timestepping based on local error tolerance
            % specified in eta
            htilde = h*(eta/(abs(vh2(1)-vs(1))/(2^p-1)))^(1/(p+1));

            if h > htilde
                h=0.9*htilde;
                i=i-1;
            else
                h=0.9*htilde;
                v(i,:) = vh2;
            end
        end

        % Find the new iteration for the temperature at tau_L and compare
        % to the chosen value of T_L (5 in this case)
        Tf  = v(end,1);
        ep  = abs(TL-Tf)/TL;

        % Save the current value of qi
        qir(p) = qi;

        % Reset qi based on its deviation from the chosen value of T_L (5
        % in this case)
        if Tf<TL
            qi=qi*(1 + .8*ep);
        else
            qi=qi*(1 - .8*ep);
        end

    end

    % Save an array of each temperature and z distribution
    T(:,1)  = v(:,1);
    zt(:,1)  = v(:,3);


    plot(zt(:),T(:),'--')
    p=p+1;
    clear T
    clear zt
```

```
end
%save(T(2,:),'Tfpd')
% Format Plots
legend('N=10^{-2}','N=10^{-1}','N=10^{0}','N=10^{1}','N=10^{2}','N=10^{3}','Location','SouthEast');
title('Rosseland Approximation for Combined Conduction and Radiation');
axis([0 tauL .5 Tf])
xlabel('Normalized Optical Thickness \tau_L/\tau');
ylabel('Dimensionless Temperature \theta');
```

F Subroutines: Heun's Method and F() for Rosseland; A(), B(), C(), and D() for RTE

```
% Jon Van Lew 2010
function [v] = huen(v1,h,N)

    v = v1 + h/2.*F(v1,N) + h/2.*F(v1 + h.*F(v1,N),N);

end

% F for the RHS of the system of ODEs in the Rosseland solution
% Jon Van Lew 2010
function yOut = F(yIn,N)

yOut(1)   =     yIn(2);
yOut(2)   =     -4*yIn(1)^2*yIn(2)^2/(N+4*yIn(1)^3/3);
yOut(3)   =     1;


% A function called by RTE tridiagonalization
% Jon Van Lew 2010
function Aout = A(x)
Aout = 1;
end

% B function called by RTE tridiagonalization
% Jon Van Lew 2010
function Bout = B(x)
Bout = 0;
end

% C function called by RTE tridiagonalization
% Jon Van Lew 2010
function Cout = C(x)
Cout = 0;
```

```
end

% D function called by RTE tridiagonalization
% Jon Van Lew 2010
function Dout = D(x,dpsidtau,N)
Dout = (1/(4*N))*dpsidtau;
end
```

References

[1] Michael F. Modest. *Radiative Heat Transfer.* Academic Press, 2003.